A 5G MIMO Antenna for Broadcast and Traffic Communication Topologies Based on Pseudo Inverse Synthesis

AHMED ALIELDIN, (Member, IEEE), **YI HUANG**, (Senior Member, IEEE), **MANOJ STANLEY,**
SUMIN DAVID JOSEPH, AND DAJUN LEI
Department of Electrical Engineering and Electronics, University of Liverpool, Liverpool L69 3GJ, U.K.

Corresponding author: Yi Huang (yi.huang@liverpool.ac.uk)

ABSTRACT This paper proposes a new design of a dual-polarized base station antenna for sub-6-GHz 5G communication covering the band from 3.3 to 3.8 GHz. The proposed antenna offers a good impedance matching across the desired frequency band with VSWR $\leq$ 1.5, a stable radiation pattern with a half power beam width of $65° \pm 5°$, and a high isolation between the ports with a small size and a low profile. The antenna is converted to a planar MIMO antenna array with low envelop correlation coefficients between the array elements to perform in either a broadcast or traffic communication topology whenever required. In the broadcast communication topology, the proposed MIMO antenna array covers a sector of $65°$ in the horizontal plane with three different down-tilted beam directions at $0°$, $10°$, and $20°$ in the vertical plane as conventional base station antennas used for 2G, 3G, and 4G. In traffic topology, the proposed MIMO antenna array can direct multiple beams to concurrent multiple users in a point-to-multipoint communication based on a novel pseudoinverse synthesis (PIS). The novel PIS is proved to be better than the other approaches which use spatial or frequency diversity as it possesses the advantage of the spatial diversity (by using a single frequency for multi-user coverage) and the advantages of the frequency diversity (by offering good steering capability and high directivity for each user). It is capable of radiating dynamic multiple beams simultaneously with an excellent flexibility and steering capability in real-time processing and outperforming other multi-beam antenna array methods. Thus, this new design is an ideal candidate for the new 5G mobile base stations.

INDEX TERMS Antenna array, base station, broadcast, dual-polarized, MIMO, pseudo inverse synthesis.

I. INTRODUCTION

As telecommunication vendors are about to introduce 5G mobile communication systems from 2019, base station and mobile antennas need to cover the new sub-6 GHz 5G frequency bands. In 2016, the European Commission (EC) announced its spectrum plan for 5G trials from 3.4 to 3.8 GHz. In 2017, the Chinese Ministry of Industry and Information Technology (MIIT) officially declared that 3.3-3.4 (indoor only), 3.4-3.6 and 4.8-5 GHz bands were allocated for 5G services [1]. For base station antennas, diversity in polarization (typically at $\pm45°$) has been used to improve the signal-to-noise ratio (SNR) and system performance [2]. Base station antennas should maintain good impedance matching within the entire frequency bands of interest, a stable radiation pattern and also a high cross polarization discrimi-

nation ratio (XPD) simultaneously [3]. XPD is defined as the power ratio between co- and cross-polarizations in two orthogonal planes (typically $\pm45°$ for base station antennas). Many successful designs have been introduced for the 2G, 3G and 4G applications using planar cross dipoles [4] or 3D printed cross dipoles [5]. Furthermore, a quite few designs have been recently introduced for the sub-6 GHz 5G applications. In [6], stacked patch antenna was used to operate at a single frequency of 3.7 GHz. In [7], an antenna based on vector synthetic mechanism was introduced with a small size and an industrial impedance matching (VSWR $\leq$ 1.5) but its bandwidth (BW) is insufficient (3.3-3.6 GHz). In [8], the BW was improved at the expense of the antenna size to meet the non-industrial impedance matching requirement (VSWR $\leq$ 2). In [9], a 2×2 antenna subarray was used to pro-

vide a high gain covering the frequency band from 3.45 GHz to 3.55 GHz. Later on, metamaterial was used to design multiband antennas as in [10] and [11] but their single polarization limits their applications in mobile communications.

Multiple-Input Multiple-Output (MIMO) is considered as a key technology for deploying the 5G network at both Sub-6 GHz and mm-wave bands. For the next few years, the Sub-6 GHz for 5G network will be in service side-by-side with the 3G and 4G networks to provide broadcast wireless mobile communications. Furthermore, 5G is expected to provide traffic communications in a point-to-multipoint (P2MP) basis [12]. Many approaches have been adopted to achieve the traffic communication topology. The most commonly used approach is applying spatial or frequency diversity to a MIMO antenna array. In spatial diversity, the MIMO array is divided into small sub-arrays each of which is fed and controlled independently to direct its beam to a user [13]. For frequency diversity, different frequencies within the 5G frequency band (with a separation of 40 MHz at least between two successive frequencies) are employed to generate different radiation patterns directed to concurrent users in a one-to-one basis [14]. The main drawbacks of the spatial diversity approach are the low directivity (user-selectivity) and the limited steering capability of the radiation pattern due to the limited sub-arrays apertures. On the other hand, although the frequency diversity approach affords high directive beams with good steering capabilities, the narrow BW limits the number of users to 10-12 at any moment per base station [15].

Another approach to achieve traffic communication topology is using multi-beam antenna arrays to generate a number of simultaneous or switchable but independent directive beams with a high gain [12], [13]. A multi-beam antenna array may use butler matrix [16]–[18] or multi-feeding ports [19], to generate concurrent but static multiple beams or digital [20] and hybrid beamforming [21] to generate dynamic but switched multiple beams. To get the advantages of having concurrent and dynamic multi-beam radiation pattern simultaneously by a single antenna array, array syntheses are applied using different optimization algorithms [22]–[27]. These algorithms need a long processing time which limits their usages in the real-time 5G applications.

Based on the above discussions, a novel dual-polarized antenna element for sub-6 GHz 5G applications is proposed in this paper. The proposed antenna element covers the frequency band from 3.3 GHz to 3.8 GHz with VSWR $\leq$ 1.5 and a good isolation between its ports (better than 25 dB). It offers a high XPD and a stable radiation pattern within its frequency band with a half power beam width (HPBW) of 65 $\pm$ 5° in addition to its small size and low profile in comparison to the reported antennas in the literature.

Another major contribution of this paper is that a 5G MMO antenna array based on the new antenna element is proposed. The proposed MIMO array offers a good diversity performance with very low envelop correlation coefficients (ECC) between its antenna elements. It offers the freedom to operate in broadcast or traffic topology. In broadcast topol-

ogy, the MIMO array covers a spatial sector of 65° and 30° in horizontal and vertical planes respectively. In traffic topology, a novel Pseudo Inverse Synthesis (PIS) is applied which has been found to enjoy the advantages of the frequency diversity approach (high directivity and good steering capability of the radiation pattern) without scarifying the advantage of the spatial diversity approach (using a single frequency for multi-user coverage). Furthermore, PIS outperforms the reported approaches in multi-beam antenna arrays as it offers simultaneous dynamic multiple beams with an excellent flexibility and steering capability in a real-time processing.

The paper is organized as follows: Section II describes the proposed antenna element, its working principles, its results and some parametrical studies; Section III discusses the proposed MIMO antenna array in the two sub-6 GHz 5G communication topologies (broadcast and traffic) with a detailed discussion on the proposed PIS and a comparison to other reported approaches. And finally, conclusions are drawn in Section IV.

II. DUAL-POLARIZED ANTENNA ELEMENT
A. ANTENNA ELEMENT DESIGN
In this section, a novel dual-polarized antenna element covering the band from 3.3 GHz to 3.8 GHz is illustrated. Fig. 1 shows the exploded geometry of the proposed design: the antenna consists of three stacked layers. Layer I (the feeding layer) is a Rogers RT5880 laminate with thickness Hd = 1.6 mm, relative permittivity ε_{r1} = 2.2 and tangential loss of 0.0009. A square feeding patch is printed on the top of Layer I with two orthogonal 50 Ω feed lines for dual-polarization which are excited by two feeding ports. A ground plane is printed on the bottom side of Layer I to provide unidirectional radiation. Layer II is a foam layer with thickness H = 9 mm and relative permittivity ε_{r2} ≈ 1. Layer III (the radiating layer) is a Rogers RT5880 laminate which has the same characteristics as Layer I. A radiating square patch, with the same dimensions as the feeding patch, is printed on the bottom side of Layer III while a parasitic copper patch is printed on the top side. Two orthogonal symmetrical rectangular slots are cut in the radiating patch. The three layers are oriented in the XY plane. The three layers, the three patches (feeding, radiating and parasitic patches) and the slots are concentric. For base station antennas, $\pm$ 45° dual-polarization is required. So, the side lengths of the layers, patches, feed lines and slots form angles of $\pm$45° with the X and Y axes respectively.

The optimized dimensions (in mm) are determined as follows: WP1 = WP2 = 27, WP3 = 20, WS1 = 71, WS2 = 30, L_Slot = 9. W_Slot = 3 and H = 9.

B. ANTENNA PRINCIPLES OF OPERATION
Two reference designs (antenna REF1 and antenna REF2) are employed to understand the working principle of the proposed antenna element as shown in Fig. 2. Initially, a single substrate (Layer I) with a square patch of $0.5\lambda_g$ in length
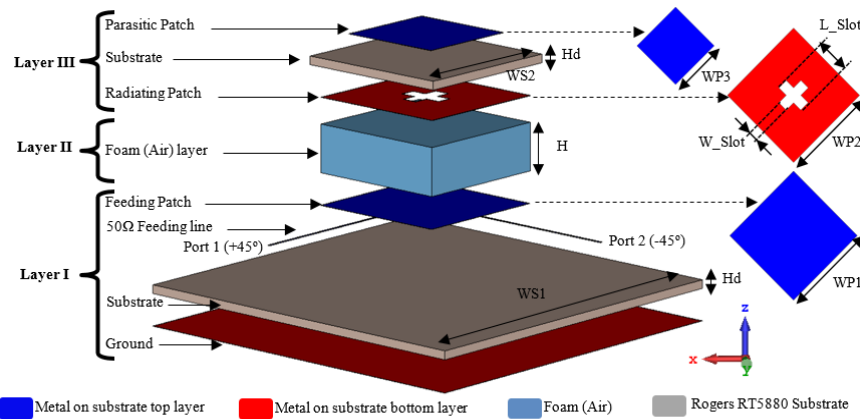
FIGURE 1. Exploded geometry of the radiating antenna element.

was designed with dual orthogonal feed lines (where λ_g is the guided wavelength at the central frequency 3.55 GHz) (antenna REF1). In this case, the BW observed is narrow. The design is amended by adding Layer II and Layer III (without the parasitic patch) above Layer I with radiating patch printed on the bottom side of Layer III. The radiating patch, in this case, is fed by the electric field coupling from Layer I. Furthermore, two rectangular slots are cut in the radiating patch to improve the impedance matching across the desired frequency band (antenna REF2). So, the BW is observed to be wider but still not satisfactory. The BW can be further improved by printing a parasitic patch on the top side of Layer III (proposed design). The parasitic patch can improve the BW by adding a capacitive loading to the antenna input impedance and hence cover the frequency band from 3.3 GHz to 3.8 GHz with a reflection coefficient ≤ -15 dB (VSWR ≤ 1.5) as shown in Fig. 2.
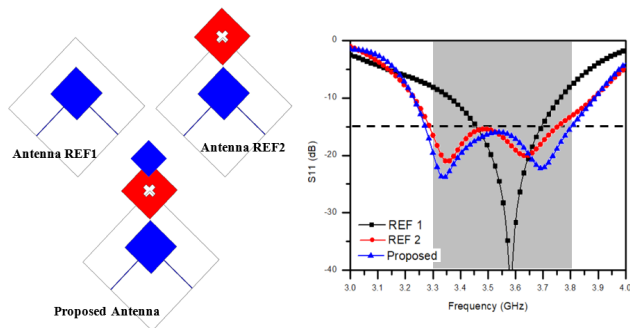

FIGURE 2. References and the proposed antenna element designs.

Fig. 3 shows the current distributions across the radiating patch at the central frequency (3.55 GHz) feeding from port 1 ($+ 45°$) and port 2 ($- 45°$). It is evident that the two current distributions are symmetrically inversed which indicates good isolation between the ports and high XPD between the co- and cross-polarized radiation patterns.

C. ANTENNA ELEMENT RESULTS
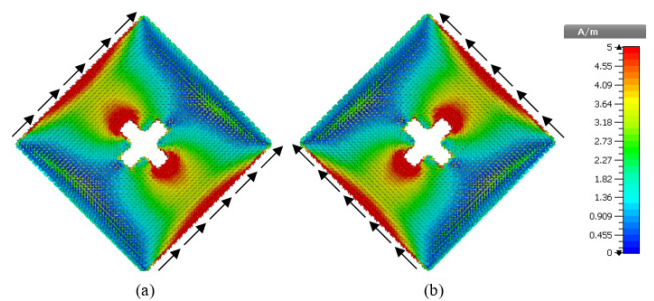To validate the proposed design, a prototype was fabricated as shown in Fig. 4, and then measured. The simulation was

FIGURE 3. The current distributions across the radiating patch at the central frequency feeding from (a) port 1 (b) port 2.
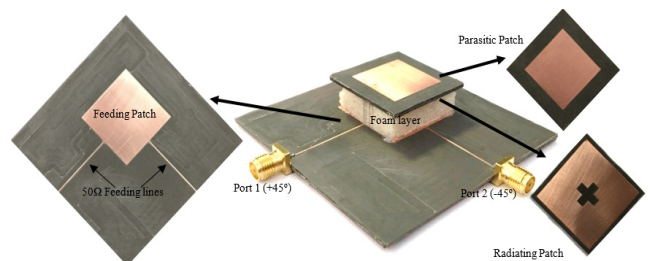

FIGURE 4. A prototype of the proposed antenna element.

accomplished by using CST microwave studio. Measured results of S-parameters, gain, and radiation patterns were obtained by using a Vector Network Analyzer (VNA) and an anechoic chamber. Fig. 5 shows a good agreement between the simulated and measured reflection coefficients, isolations between the ports and realized gains. A fractional BW of 14% is achieved (3.3-3.8 GHz) with VSWR ≤ 1.5 to meet the standard industrial requirements. The measured port-to-port isolation is better than 25 dB across the operating frequency band. It is apparent also that the proposed antenna has a stable realized gain of 8.5 ± 0.5 dBi across the frequency band of interest.

The measured co-and cross-polarized radiation patterns at the start, central and stop frequencies in H-plane (XZ plane) and V-plane (YZ plane) are shown in Fig. 6. Because the structure is almost symmetrical around the X and Y axes, the HPBWs in H-plane and V-plane are about $65 \pm 5°$ across
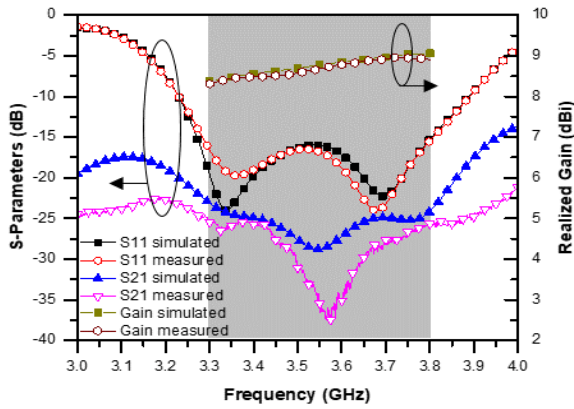
FIGURE 5. Simulated and measured reflection coefficients, isolations between the ports and realized gains.
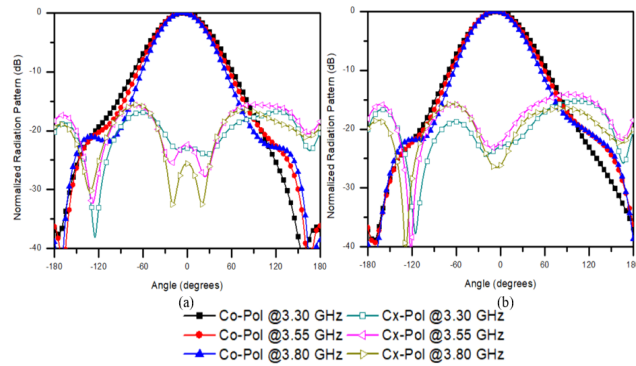

FIGURE 6. Normalized measured radiation patterns in (a) H-plane (b) V-plane.

the frequency band. The XPD is better than 22 dB at boresight and better than 8 dB within a sector of $\pm\,60°$.

A comparison between the state-of-the-art sub-6 GHz 5G antennas reported in the literature and the proposed antenna is tabulated in Table I. It is apparent that the proposed antenna design has the widest BW with the industrial standard VSWR $\leq$ 1.5, a small size, a high gain with a good isolation between its ports and a high XPD.

TABLE 1. Comparison of reported SUB-6 Ghz 5G base station antennas to the proposed antenna.

Ref.	[6]	[7]	[9]	Proposed
Frequency (GHz)	3.65-3.81	3.3-3.6	3.45-3.55	**3.3-3.8**
Size (mm³)	86×81×3	72×72×18.8	74×74×1.5	**71×71×12.2**
Isolation (dB)	31	28.8	15	**25**
Average gain (dBi)	10	8.2	8	**8.8**
Polarization	Dual	Dual	Single	**Dual**
XPD (dB)	23	24	NA	**22**

D. PARAMETRIC STUDY
An important parameter in the design is the height of the gap H between the feeding and the radiating layers which

determines the coupling between these two layers and hence affects the input impedance of the antenna. When H is smaller, the feeding layer gets closer to the radiating layer and the input impedance becomes more capacitive and vice versa as shown in the Smith chart in Fig. 7. For optimum impedance matching, H should be 9 mm to achieve VSWR $\leq$ 1.5 (the purple circle at the middle of the Smith chart) within the desired frequency band.
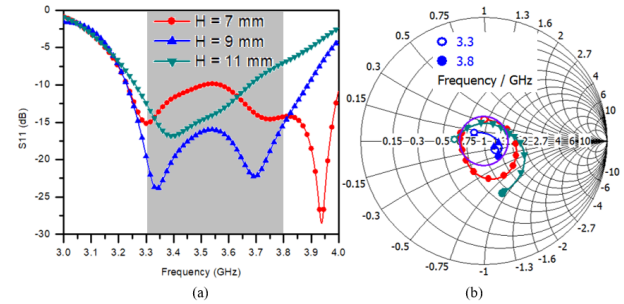

FIGURE 7. Effect of H on the reflection coefficient illustrated by (a) S-parameters (b) Smith chart.

The second parameter studied was the length of the slots L_Slot in the radiating patch. It controls the input impedance of the radiating patch seen from the feeding points. The slot length L_Slot is optimized and set to be 9 mm to cover the frequency band from 3.3 GHz to 3.8 GHz with a reflection coefficient better than -15 dB as shown in Fig. 8.
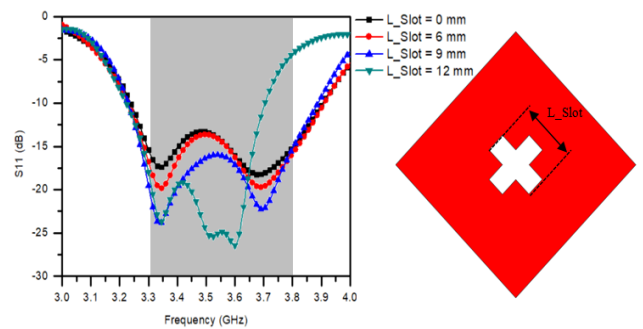

FIGURE 8. Effect of L_Slot on the reflection coefficient.

The third parameter studied was the side length of the parasitic patch $WP3$. It affects the amount of the capacitive loading added to the antenna input impedance. The larger the parasitic patch, the higher capacitive loading is added. $WP3$ is set to 20 mm for optimum impedance matching across the desired frequency band as presented in Fig. 9.

III. MIMO ANTENNA ARRAY
In this section, a dual-polarized MIMO antenna array based on the antenna element presented in Section II is designed to operate in one of the two different communication topologies used in 5G mobile communications (broadcast and traffic). In the broadcast topology, the 5G base station antenna array is required to perform as conventional directive 2G, 3G and
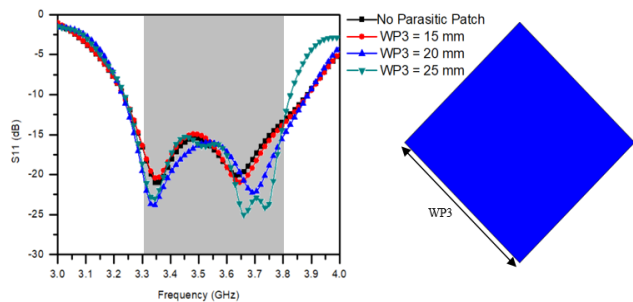
FIGURE 9. Effect of *WP3* on the reflection coefficient.

4G base station antennas covering a sector in a hexagonal cellular mobile network with a horizontal HBPW of 65° and a vertical down tilting from 0° to 20°. On the other hand, in the traffic topology, the 5G base station antenna is required to communicate with concurrent users in a P2MP communication by assigning multiple beams with narrow HPBWs to multiple users (typically one beam for each user). Switching between these topologies (broadcast and traffic) depends on the excitation scenarios of the antenna elements in the MIMO array.

Fig. 10 presents the MIMO antenna array structure. It consists of 27 elements (3 columns and 9 rows). The spacing between two successive columns is set to 65 mm ($0.8\lambda_0$) while the spacing between two successive rows is set to 50 mm ($0.6\lambda_0$) (where λ_0 is the free space wavelength at the central frequency 3.55 GHz). To identify the location of an antenna element in the array easily, the columns are numbered as C1, C2 and C3 from left to right while the rows are numbered as R1 to R9 from up to down as shown in Fig. 10.
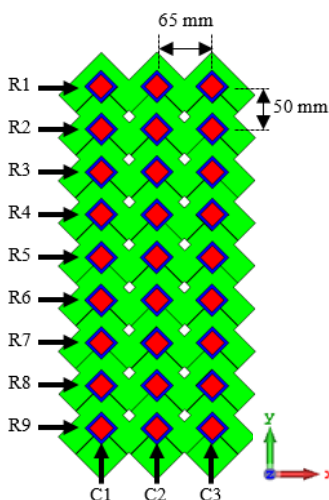

FIGURE 10. The structure of the proposed MIMO antenna array.

To evaluate the diversity performance of the proposed MIMO array, the ECC can be obtained from the spherical

mode spectrum of the antenna as [28]:

$$ECC = \frac{\sum_{l=1}^{\infty} \sum_{m=-1}^{l} \sum_{s=1}^{2} q_{sml}^{1}(q_{sml}^{2})^{*}}{\sqrt{(\sum_{l=1}^{\infty} \sum_{m=-1}^{l} \sum_{s=1}^{2} q_{sml}^{1}(q_{sml}^{1})^{*})(\sum_{l=1}^{\infty} \sum_{m=-1}^{l} \sum_{s=1}^{2} q_{sml}^{2}(q_{sml}^{2})^{*})}} \tag{1}$$

where q_{sml} is the complex coefficient of the spherical harmonic, the order m ($-l \leq m \leq l$) describes the azimuthal variation of the field, the variation in elevation depends on the degree l and the order m, the index $s \in \{1, 2\}$ is connected with the components of transversal electric and transversal magnetic waves and $(\cdot)^{*}$ stands for the complex conjugate. Using equation (1), ECC is calculated and plotted in Fig. 11. Results show that the proposed MIMO array offer very low ECC. The maximum ECC is less than 0.004 across the operating frequency band, far less than the general criteria of ECC < 0.3. The two communication topologies are described in detail as follow.
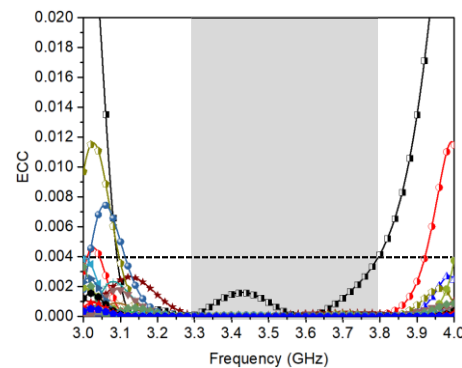

FIGURE 11. ECC of the ports of the proposed MIMO antenna array.

A. BROADCAST COMMUNICATION TOPOLOGY

In the broadcast communication topology, the MIMO antenna array is divided horizontally into three vertical linear sub-arrays; C1, C2 and, C3 as shown in Fig. 12(a). Each linear sub-array consists of 9 antenna elements. The excitation signals for each sub-array are set such that the radiated main lobes are directed to 0° (boresight), −10° and −20° for C1, C2 and C3 respectively. The negative sign at each angle indicates that the main lobe is tilted downwards. Each sub-array has a vertical HPBW of 10°. So, the three main lobes cover a vertical sector from +5° to −25° contiguously without overlapping or gaps (from +5° to −5° by C1, from −5° to −15° by C2 and from −15° to −25° by C3) as shown in Fig. 12(b). It worth noting that the horizontal HPBW of each radiation pattern is almost the same as the single antenna element. Because the three main lobes are contiguous in the V-plane without overlapping, they almost do not interfere in the H-plane. So, the combined radiation pattern also has the same horizontal HPBW as the single antenna element. The combined radiation pattern of the three sub-arrays covers a
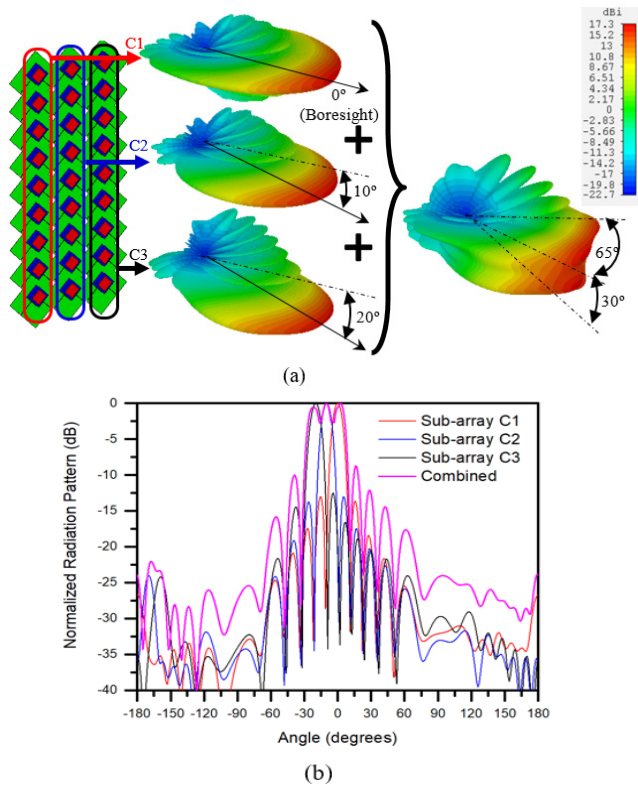
(a)

(b)

FIGURE 12. The broadcast communication topology illustrated by (a) 3D radiation patterns (b) V-plane.
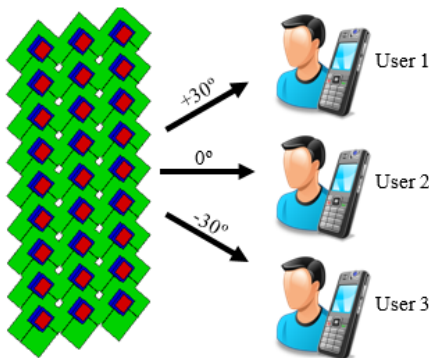

FIGURE 13. A P2MP communication scenario for three users.

solid sector with a horizontal and vertical HPBWs of 65° and 30° respectively.

B. TRAFFIC COMMUNICATION TOPOLOGY

Generally, in traffic communication topology, a spatial or frequency diversity approach is commonly used. The approach of using a multi-beam array is also applied. In this section, a multi-beam antenna array based on PIS is proposed. The spatial and frequency diversities for the same MIMO antenna array structure are illustrated to show how the proposed PIS can overcome the drawbacks of spatial and frequency diversities.
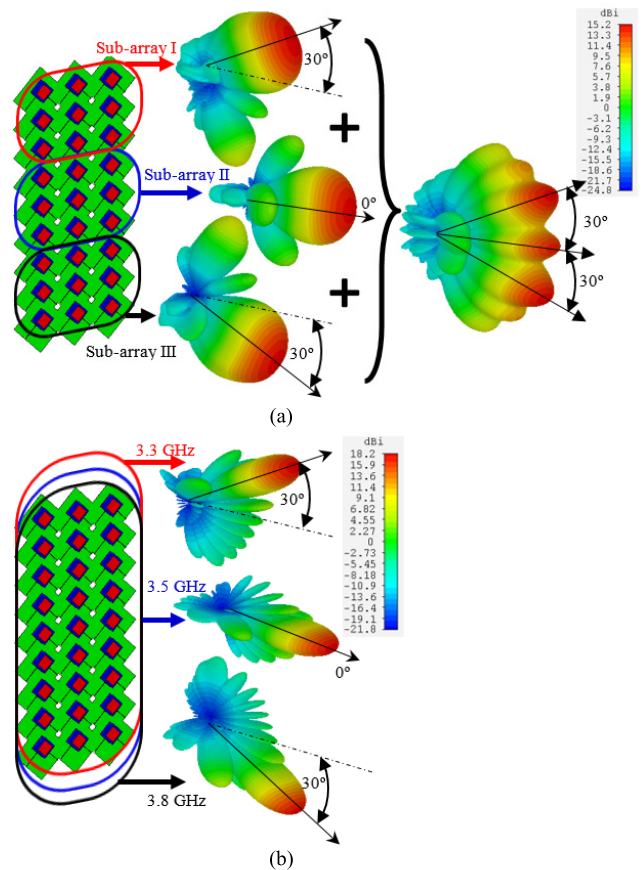

(a)

(b)

FIGURE 14. The traffic communication topology using (a) spatial diversity (b) frequency diversity.

A P2MP communication scenario is assumed in this paper where three users are located at three different angles (+30°, 0° and −30° respectively) as shown in Fig. 13. For the spatial diversity approach, the MIMO array is divided vertically into three planar 3 × 3 sub-arrays. Sub-array I (consists of R1, R2 and R3), sub-array II (consists of R4, R5 and R6) and sub-array III (consists of R7, R8 and R9) as shown in Fig. 14(a). The three sub-arrays operate at the same frequency and the excitation signals of each sub-array are set independently to direct its main lobe to one of the users on a one-to-one basis. From the combined radiation pattern shown in Fig. 14(a), we can see that there are two main drawbacks in the spatial diversity approach. The first drawback is that the combined radiation pattern has overlapped the main lobes due to their low directivity (selectivity) toward the users because the sub-arrays aperture is limited. The second drawback is the limited capability of beam steering of each sub-array due to the limitation in the sub-array aperture.

For the frequency diversity approach, the whole MIMO antenna array is excited by signals at three different frequencies (3.3 GHz, 3.5 GHz and 3.8 GHz) as shown in Fig. 14(b). First, the phases of the signal at each frequency are adjusted to direct the main lobe of the radiation pattern at this frequency to one of the users in a one-to-one basis then the

three signals are superimposed and fed to the MIMO array. From the radiation patterns shown in Fig. 14(b) we notice that the frequency diversity approach overcomes the drawbacks of the spatial diversity approach as it offers high directivity and good steering capability because it uses the whole array aperture. On the other hand, the disadvantage of the frequency diversity approach is using a single frequency for each user instead of using a single frequency for multi-user which is considered as an advantage in the spatial diversity approach. The separation between the frequencies should be 40 MHz at least [14]. This limits the number of users served by the base station antenna due to the limited spectrum of the 5G.

Multi-beam antenna arrays may also be used to serve multi-users in traffic communication topology. One of the methods used in multi-beam antenna arrays is the simultaneous static multi-beam approach using a Butler matrix or multiple feeding ports. The drawbacks of this method are the limited steering capability of the static multi-beam which does not meet the requirements for 5G mobile applications and that the more beams are required, a more complicated feeding network is needed. Another method used in multi-beam arrays is using digital, analog or hybrid beamforming technique which allows dynamic but switchable (not simultaneous) multiple beams. Again, not applicable for concurrent user service. Another method used in multi-beam antenna arrays is using optimization algorithms to synthesize multi-beam radiation patterns. Although the radiation patterns, in this case, may have simultaneous and dynamic multiple beams, they need long processing time which is not applicable for real-time 5G applications.

To understand how the proposed PIS works, we first study the general formula of the radiation pattern formed by a planar antenna array in the XY plane. The radiation pattern $P(\theta, \phi)$ can be found by multiplying the ($MN \times 1$) complex weight vector W_{mn} by the ($MN \times LP$) steering matrix $A(\theta, \phi)$ [29]

$$P(\theta, \emptyset) = W_{mn}^H \times A(\theta, \emptyset) \qquad (2)$$

where

$$W_{mn} = [w_{11}, w_{21}, \ldots, w_{M1}, w_{12}, \ldots, w_{MN}]^T \qquad (3)$$

$$A(\theta, \emptyset) = [a_{11}(\theta, \emptyset), a_{21}(\theta, \emptyset), \ldots, a_{M1}(\theta, \emptyset),$$
$$a_{12}(\theta, \emptyset), \ldots, a_{MN}(\theta, \emptyset)]^T \qquad (4)$$

$$a_{mn}(\theta, \emptyset) = [e^{-iksin(\theta_1)[(m-1)d_x\cos(\emptyset_1)+(n-1)d_y\sin(\emptyset_1)]}, \ldots,$$
$$e^{-iksin(\theta_L)[(m-1)d_x\cos(\emptyset_1)+(n-1)d_y\sin(\emptyset_1)]}, \ldots,$$
$$e^{-iksin(\theta_L)[(m-1)d_x\cos(\emptyset_P)+(n-1)d_y\sin(\emptyset_P)]}] \qquad (5)$$

$(\cdot)^T$ and $(\cdot)^H$ stand for the transpose and Hermitian transpose, M and N are the total numbers of the array rows and columns, θ and ϕ are the aspect angles in the XZ and YZ planes measured from the antenna array boresight, L and P are the

numbers of the defined aspect angles θ and ϕ, dx and dy are the separations between two successive antenna elements in the X-axis and Y-axis respectively, w_{mn} is the complex weight of the antenna element number mn, k is the angular wave number which equals to $2\pi/\lambda$ and λ is the free space wavelength.

If we consider $P_d(\theta, \phi)$ as a pre-defined radiation pattern at each value of θ and ϕ, the corresponding synthesized complex weight vector W_{mns} can be found by substituting in equation (2) to yield

$$W_{mns}^H = P_d(\theta, \emptyset) \times [A(\theta, \emptyset)]^{-1} \qquad (6)$$

To obtain the inverse of the steering matrix $A(\theta, \phi)$ using classical mathematics, $A(\theta, \phi)$ should be a non-singular square matrix (i.e. $MN = LP$). So, we have two cases.

Case (1): the number of the array elements MN should be as large as the number of the defined aspect angles LP which will result in an extremely large array (not practical).

Case (2): the number of the defined aspect angles LP is as limited as the number of the array elements MN which results in a radiation pattern with a poor resolution.

To solve this problem, pseudo (Moore–Penrose) inverse matrix is used to obtain the inverse of $A(\theta, \phi)$. Thus, from equation (6), PIS is defined as

$$W_{mns}^H = P_d(\theta, \emptyset) \times \left[A^H(\theta, \emptyset) \times \left(A(\theta, \emptyset) \times A^H(\theta, \emptyset)\right)^{-1}\right] \qquad (7)$$

By applying PIS in equation (7) to a pre-defined radiation pattern $P_d(\theta, \phi)$ with three narrow main lobes at $-30°$, $0°$ and $30°$ to match the requirements of the P2MP communication scenario presented in Fig. 13, the corresponding synthesized complex weight vector W_{mns} can be determined as shown in Table II. The weight vector tabulated in Table II is applied to the proposed MIMO antenna array and the simulated 3D radiation pattern is presented in Fig. 15(a).

TABLE 2. Synthesized complex weight vector W_{mns} using PIS.

Antenna Elements		R1	R2	R3	R4	R5	R6	R7	R8	R9
Complex weight	Attenuation (dB)	0	16	13	1.5	4.3	10	7	0.6	19
	Phase (º)	0	0	180	0	0	180	0	0	180

It is clear that PIS has overcome the disadvantages of both the frequency and spatial diversity approaches as it can cover the three users simultaneously at a single frequency with a high directivity (a narrow beam width) and good steering capability. It can also generate a radiation pattern with simultaneous and dynamic multiple beams in a real-time processing. From Fig. 15(b), it is evident that the pre-defined and the simulated radiation patterns have a

TABLE 3. Comparison of the proposed PIS to other reported approaches.

| Method	Frequency	Directivity	Steering Capability	Simultaneousness	Real-time
Spatial Diversity	Single	Low	Low	Yes	Yes
Frequency Diversity	Multiple	High	High	Yes	Yes
Simultaneous Multi-beam [16]-[17]-[18]-[19]	Single	High	Static	Yes	Yes
Switchable Multi-beam [20]-[21]	Single	High	High	No	Yes
Optimized Multi-beam [24]-[25]-[26]-[27]	Single	High	High	Yes	No
PIS	**Single**	**High**	**High**	**Yes**	**Yes**
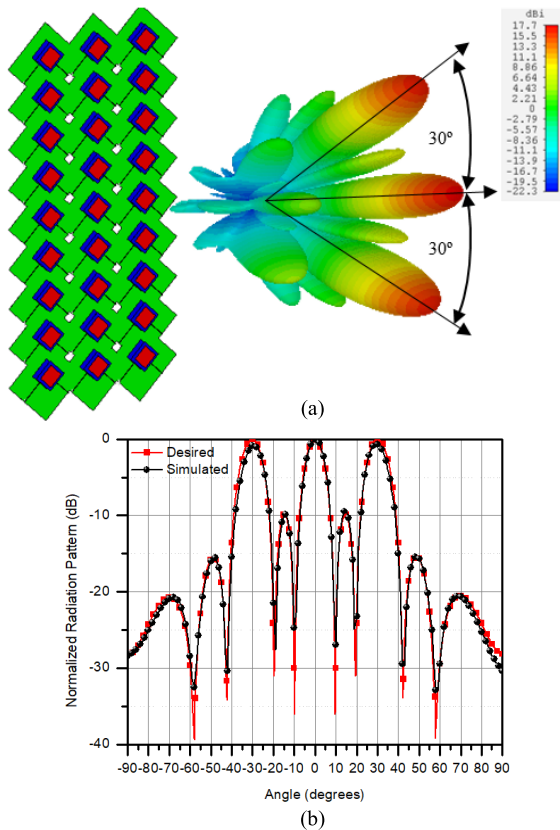
FIGURE 15. The traffic communication topology using the proposed PIS illustrated by (a) 3D radiation patterns (b) V-plane.

good agreement which indicates how accurate the PIS is. Table III compares the different approaches used in the literature with the proposed PIS. It is clear that the proposed PIS overcomes the drawbacks found in other approaches as PIS can generate a simultaneous dynamic multi-beam radiation pattern with a high directivity and a good steering capability at a single frequency in a real-time processing outperforming other multi-beam antenna array methods (while the frequency diversity approach uses multiple frequencies). Furthermore, the number of users served by the MIMO 5G base station can be increased by applying PIS at multiple frequencies.

IV. CONCLUSION

A new dual-polarized base station antenna has been designed, optimized, fabricated and measured for the sub-6 GHz 5G applications. The proposed design covers a frequency band from 3.5 GHz to 3.8 GHz with industrial impedance matching specification (VSWR $\leq$ 1.5) and good isolation between its ports. It also has a stable radiation pattern within the desired frequency band with a small size and low profile in comparison to other reported designs. A MIMO antenna array based on the antenna element has been proposed to perform in one of the two 5G communication topologies (broadcast and traffic). A novel PIS has been illustrated and applied to the proposed MIMO array for the traffic topology. It has been shown that PIS offers the advantages of both the frequency and spatial diversity approaches as it uses a single frequency to generate multiple beams with high directivity and good steering capability. PIS has also been shown outperforming other multi-beam antenna array methods as it is capable of radiating simultaneous dynamic multiple beams in a real-time processing which makes the proposed design an ideal antenna candidate for the sub-6 GHz 5G base stations.

REFERENCES

[1] *Ministry of Industry and Information Technology of China [EB/OL]*. Accessed: Oct. 1, 2018. [Online]. Available: http://www.miit.gov.cn/n1146290/n4388791/c5906943/content.html

[2] X.-P. Mao and J. W. Mark, "On polarization diversity in mobile communications," in *Proc. Int. Conf. Commun. Technol.*, Guilin, China, 2006, pp. 1–4.

[3] Q.-X. Chu, Y. Luo, and D.-L. Wen, "Three principles of designing base-station antennas," in *Proc. Int. Symp. Antennas Propag. (ISAP)*, Hobart, TAS, Australia, Nov. 2015, pp. 1–3.

[4] A. Alieldin and Y. Huang, "Design of broadband dual-polarized oval-shaped base station antennas for mobile systems," in *Proc. IEEE Int. Symp. Antennas Propag. USNC/URSI Nat. Radio Sci. Meeting*, San Diego, CA, USA, Jul. 2017, pp. 183–184.

[5] H. Huang, Y. Liu, and S. Gong, "A dual-broadband, dual-polarized base station antenna for 2G/3G/4G applications," *IEEE Antennas Wireless Propag. Lett.*, vol. 16, pp. 1111–1114, 2017.

[6] Y. Gao, R. Ma, Y. Wang, Q. Zhang, and C. Parini, "Stacked patch antenna with dual-polarization and low mutual coupling for massive MIMO," *IEEE Trans. Antennas Propag.*, vol. 64, no. 10, pp. 4544–4549, Oct. 2016.

[7] H. Huang, X. Li, and Y. Liu, "5G MIMO antenna based on vector synthetic mechanism," *IEEE Antennas Wireless Propag. Lett.*, vol. 17, no. 6, pp. 1052–1055, Jun. 2018.

[8] Q. Wu, P. Liang, and X. Chen, "A broadband ±45° dual-polarized multiple-input multiple-output antenna for 5G base stations with extra decoupling elements," *J. Commun. Inf. Netw.*, vol. 3, no. 1, pp. 31–37, Mar. 2018.

[9] M. A. Al-Tarifi, M. S. Sharawi, and A. Shamim, "Massive MIMO antenna system for 5G base stations with directive ports and switched beam-steering capabilities," *IET Microw., Antennas Propag.*, vol. 12, no. 10, pp. 1709–1718, Aug. 2018.

[10] M. Alibakhshi-Kenari, M. Naser-Moghadasi, R. A. Sadeghzadeh, B. S. Virdee, and E. Limiti, "Periodic array of complementary artificial magnetic conductor metamaterials-based multiband antennas for broadband wireless transceivers," *IET Microw., Antennas Propag.*, vol. 10, no. 15, pp. 1682–1691, Dec. 2016.

[11] M. Alibakhshikenari, B. S. Virdee, A. Ali, and E. Limiti, "Miniaturised planar-patch antenna based on metamaterial L-shaped unit-cells for broadband portable microwave devices and multiband wireless communication systems," *IET Microw., Antennas Propag.*, vol. 12, no. 7, pp. 1080–1086, Jun. 2018.

[12] Z. Wu, B. Wu, Z. Su, and X. Zhang, "Development challenges for 5G base station antennas," in *Proc. Int. Workshop Antenna Technol. (iWAT)*, Nanjing, China, 2018, pp. 1–3.

[13] D. Muirhead, M. A. Imran, and K. Arshad, "A survey of the challenges, opportunities and use of multiple antennas in current and future 5G small cell base stations," *IEEE Access*, vol. 4, pp. 2952–2964, 2016.

[14] E. Björnson, L. Van der Perre, S. Buzzi, and E. G. Larsson. (Mar. 2018). "Massive MIMO in sub-6 GHz and mmWave: Physical, practical, and use-case differences." [Online]. Available: https://arxiv.org/abs/1803.11023

[15] H. Hu, H. Gao, Z. Li, and Y. Zhu, "A sub 6 GHz massive MIMO system for 5G new radio," in *Proc. IEEE 85th Veh. Technol. Conf. (VTC Spring)*, Sydney, NSW, Australia, Jun. 2017, pp. 1–5.

[16] H.-T. Chou, "An effective design procedure of multibeam phased array antennas for the applications of multisatellite/coverage communications," *IEEE Trans. Antennas Propag.*, vol. 64, no. 10, pp. 4218–4227, Oct. 2016.

[17] Y. Cao, K.-S. Chin, W. Che, W. Yang, and E. S. Li, "A compact 38 GHz multibeam antenna array with multifolded butler matrix for 5G applications," *IEEE Antennas Wireless Propag. Lett.*, vol. 16, pp. 2996–2999, 2017.

[18] Q. Wu, J. Hirokawa, J. Yin, C. Yu, H. Wang, and W. Hong, "Millimeter-wave multibeam endfire dual-circularly polarized antenna array for 5G wireless applications," *IEEE Trans. Antennas Propag.*, vol. 66, no. 9, pp. 4930–4935, Sep. 2018.

[19] J. Zhang, W. Wu, and D.-G. Fang, "360° scanning multi-beam antenna based on homogeneous ellipsoidal lens fed by circular array," *Electron. Lett.*, vol. 47, no. 5, pp. 298–300, Mar. 2011.

[20] A. S. Daryoush, "Digitally beamformed multibeam phased array antennas for future communication satellites," in *Proc. IEEE Radio Wireless Symp.*, Orlando, FL, USA, Jan. 2008, pp. 831–834.

[21] S. Mondal, R. Singh, A. I. Hussein, and J. Paramesh, "A 25–30 GHz fully-connected hybrid beamforming receiver for MIMO communication," *IEEE J. Solid-State Circuits*, vol. 53, no. 5, pp. 1275–1287, May 2018.

[22] M. A. Panduro and C. del Rio-Bocio, "Design of beam-forming networks for scannable multi-beam antenna arrays using corps," *Prog. Electromagn. Res.*, vol. 84, pp. 173–188, 2008.

[23] L. Manica, P. Rocca, G. Oliveri, and A. Massa, "Synthesis of multi-beam sub-arrayed antennas through an excitation matching strategy," *IEEE Trans. Antennas Propag.*, vol. 59, no. 2, pp. 482–492, Feb. 2011.

[24] J.-S. Sheu, W.-H. Sheen, and T.-X. Guo, "On the design of downlink multiuser transmission for a beam-group division 5G system," *IEEE Trans. Veh. Technol.*, vol. 67, no. 8, pp. 7191–7203, Aug. 2018.

[25] K. R. Mahmoud and A. M. Montaser, "Performance of tri-band multi-polarized array antenna for 5G mobile base station adopting polarization and directivity control," *IEEE Access*, vol. 6, pp. 8682–8694, 2018.

[26] H.-T. Chou and J. W. Liu, "Synthesis and characteristic evaluation of convex metallic reflectarray antennas to radiate relatively orthogonal multi-beams," *IEEE Trans. Antennas Propag.*, vol. 66, no. 8, pp. 4008–4016, Aug. 2018.

[27] A. Smida, R. Ghayoula, and A. Gharsallah, "Beamforming multibeam antenna array using Taguchi optimization method," in *Proc. 2nd World Symp. Web Appl. Netw. (WSWAN)*, Sousse, Tunisia, 2015, pp. 1–4.

[28] R. Cornelius, A. Narbudowicz, M. J. Ammann, and D. Heberling, "Calculating the envelope correlation coefficient directly from spherical modes spectrum," in *Proc. 11th Eur. Conf. Antennas Propag. (EUCAP)*, Paris, France, 2017, pp. 3003–3006.

[29] N. El-Din Ismail, S. H. Mahmoud, A. Hamed, and A. Hafez, "Design and analysis of planar phased MIMO antenna for radar applications," in *Proc. Prog. Electromagn. Res. Symp. PIERS*, Guangzhou, China, vol. 28, Aug. 2014, pp. 1832–1838.

AHMED ALIELDIN received the B.Sc. degree in radar engineering from the Military Technical College, Egypt, in 2005, and the M.Sc.(Eng.) degree in antenna and microwave propagation from the University of Alexandria, Egypt, in 2013. He is currently pursuing the Ph.D. degree in electrical engineering with the University of Liverpool, U.K. He was a Radar Engineer with MoD, Egypt, and a Lecturer Assistant with the Air Defence College, Egypt. He was also an Antenna Engineer with Benha Electronics Company, where he was involved in projects of national importance. His research interests include mobile base station antennas, satellite antennas, multiple-input multiple-output (MIMO), and phased-MIMO radar antenna arrays design.

YI HUANG (S'91–M'96–SM'06) received the B.Sc. degree in physics and the M.Sc.(Eng.) degree in microwave engineering from Wuhan University, Wuhan, China, and the D.Phil. degree in communications from the University of Oxford, Oxford, U.K., in 1994.

He was a Radar Engineer with NRIET, Nanjing, China. He was a Research Staff Member with the University of Birmingham, Birmingham, U.K.; the University of Oxford; and the University of Essex. In 1994, he joined British Telecom Labs, London, U.K., as a Research Fellow. In 1995, he joined the Department of Electrical Engineering and Electronics, University of Liverpool, as a Lecturer, where he is currently the Chair of wireless engineering, the Deputy Head of the department, the Head of the High-Frequency Engineering Research Group, and the M.Sc. Program Director. He has authored over 300 refereed papers in leading international journals and conference proceedings, and authored books *Antennas: From Theory to Practice* (John Wiley, 2008) and *Reverberation Chambers* (Wiley, 2016). His current research interests include radio communications, applied electromagnetics, and radar and antennas since 1987.

He received many research grants from research councils, government agencies, charity, EU, and industry. He was a Consultant to various companies, and served for a number of the national and international technical committees (such as IET, EPSRC, European ACE, COST-IC0603, and COST-IC1102 and EurAAP). He is an Editor, an Associate Editor, and a Guest Editor of four of international journals. He is a Keynote/Invited Speaker and an Organizer of many conferences and workshops (e.g., IEEE iWAT, WiCom, and LAPC). He is currently an Editor-in-Chief of *Wireless Engineering and Technology* (ISSN 2152-2294/2152-2308), an Associate Editor of the IEEE Antennas and Wireless Propagation Letters, a College Member of EPSRC, a U.K./Ireland Delegate to EurAAP, and a fellow of the IEE/IET.

MANOJ STANLEY received the B.Tech. degree in electronics and communication from Kerala University, India, in 2012, and the M.Tech. degree in communication systems from the Visvesvaraya National Institute of Technology, India, in 2014. He is currently pursuing the Ph.D. degree in electrical engineering with the University of Liverpool, U.K. He was a Lab Engineer with the Visvesvaraya National Institute of Technology, under CoE, where he was involved in projects of national importance. His research interests include mobile phone antenna design, theory of characteristic modes, multiple-input multiple-output, and mm-wave antenna array design for 5G smartphones.

SUMIN DAVID JOSEPH received the B.Tech. degree (Hons.) in electronics and communication from the Cochin University of Science and Technology, India, in 2012, and the M.Tech. degree (Hons.) in communication systems from the Visvesvaraya National Institute of Technology, India, in 2015. He is currently pursuing the dual Ph.D. degree in electrical engineering with the University of Liverpool, U.K., and National Tsing Hua University, Taiwan.

He was a Lab Engineer with the Visvesvaraya National Institute of Technology, under CoE, where he was involved in projects of national importance. His research interests include self-biased circulators, mm-wave antenna arrays, rectifying antennas, rectifiers, wireless power transfer, and energy harvesting.

DAJUN LEI received the B.S. degree from Hunan Normal University in 1996 and the Ph.D. degree from Hunan University, Changsha, China, in 2011. He is currently a Professor with the School of Electronic Information and Electrical Engineering, Xiangnan University, Chenzhou. He also holds a visiting position with the Department of Electrical Engineering and Electronics, University of Liverpool, U.K.

His research interests are mainly in the fields of dielectric resonator microwave components and planar antennas and arrays.

• • •